Original Paper

Thermal behaviour of glass batch on batch heating

Anne J. Faber, Ruud G. C. Beerkens and Henk de Waal
TNO Institute of Applied Physics, Eindhoven (NL)

The heating process of a barium–strontium glass batch has been studied in a 40 l pot furnace, using a multiple thermocouple assembly. The effect of several batch batch parameters on the heating process has been measured, including layer thickness, cullet fraction, water content and pellets. The results have been evaluated using a heat penetration batch model. In the model two heating stages, below and above a certain batch transition temperature ϑ_s, typically 800 to 900 °C, are distinguished. Values for the temperature-dependent thermal diffusivity of the batch have been derived from experimental temperature distributions in the batch during heating. Below ϑ_s the thermal diffusivity has an almost constant value of $0.4 \cdot 10^{-6}$ m²/s for a standard (powder) batch blanket; for $\vartheta > \vartheta_s$ the net thermal diffusivity strongly increases with temperature, due to the formation of primary melt phases. For $\vartheta_s < \vartheta < 1100$ °C the average value is about $1.4 \cdot 10^{-6}$ m²/s. A 100 % cullet layer has a 50 % higher thermal diffusivity for $\vartheta < \vartheta_s$; pelletizing the batch is of little influence on the virtual thermal diffusivity and (extra) wetting has a retarding effect on batch heating due to extra heat absorption. As for the furnace temperatures it appears that increasing the temperature of the glass melt is more effective for improving the batch heating rate than increasing the temperature of the combustion chamber. Practical recommendations are given for batch preparation, charging and heating in industrial glass tanks.

Thermisches Verhalten des Glasgemenges beim Aufwärmprozeß

Es wird der technische Aufwärmprozeß eines Barium–Strontium-Glasgemenges in einem 40-l-Hafenofen unter Verwendung eines mit zahlreichen Thermoelementen ausgestatteten Meßkopfes untersucht. Der Einfluß der verschiedenen Gemengeparameter, wie z. B. die Höhe der Gemengedecke, der Scherbenanteil, die Feuchte und die Pelletierung, auf die Aufwärmung des Glasgemenges wurde untersucht. Die Ergebnisse sind mit Hilfe eines Wärmeeindringmodells für das Gemenge überprüft worden. In diesem Modell wird zwischen zwei Stufen unterschieden: unterhalb einer bestimmten Gemengeumwandlungstemperatur ϑ_s, ungefähr bei 800 bis 900 °C, und oberhalb dieser Temperatur. Die Werte für die temperaturbedingte thermische Diffusion sind von den experimentellen Temperaturverteilungen im Gemenge während der Aufwärmung des Gemenges abgeleitet worden. Die thermische Diffusion für eine normale Gemengedecke hat unterhalb ϑ_s einen konstanten Wert von $0{,}4 \cdot 10^{-6}$ m²/s. Mit steigender Temperatur $\vartheta > \vartheta_s$ nimmt die thermische Diffusion deutlich zu, verursacht durch die Bildung von primären Schmelzphasen. Der Mittelwert zwischen ϑ_s und 1100 °C ist ungefähr $1{,}4 \cdot 10^{-6}$ m²/s. Eine reine Gemengedecke aus Scherben zeigt eine 50 % höhere thermische Diffusion unterhalb ϑ_s. Der Einfluß der Pelletierung auf den Wärmetransport im Gemenge ist gering, und der Einsatz von Gemengefeuchte verzögert den Aufwärmprozeß des Gemenges durch die zusätzlich erforderliche Verdampfungswärme. Aus der Betrachtung der Ofentemperaturen geht hervor, daß bei zunehmender Temperatur der Glasschmelze bzw. des Oberofens das Gemenge stärker durch die der Schmelze und weniger durch die des Oberofens aufgeheizt wird. Zum Schluß werden einige praktische Hinweise gegeben für die Gemengeaufbereitung, das Einlegen und die Feuerung von großtechnischen Schmelzöfen.

1. Introduction

Knowledge of the thermal behaviour of glass batch is of great importance for optimization of the glass melting process. However, relatively few studies are known, that report experimentally verified descriptions of batch heating (see [1 to 4]). The objective of this study is to experimentally determine the thermal characteristics of glass batch, like heating rate and effective thermal diffusivity and to describe the thermal behaviour in a semi-empirical model.

The heating of barium–strontium glass batch was studied in a laboratory glass furnace, consisting of an electrically heated 40 l ceramic open pot, additionally fired by a gas burner from above the surface. By varying several batch parameters including layer thickness, cullet fraction and water content, the influence of these parameters on batch heating has been investigated.

The minimum (inner) temperature of a batch layer is described by a model, in which the batch layer is considered as an infinite slab, heated from two sides. In the model two heating stages, below and above a certain batch transition temperature (typically 800 to 900 °C), are distinguished. Below the batch transition temperature the heat flow through the batch is governed by the thermal diffusivity of the (powder) layer. Above the batch transition temperature, low-melting glassy phases also contribute to the net thermal diffusivity.

The relation of the batch heating model to melting kinetic models is indicated qualitatively. By combining the experimental data and the batch model, important conclusions can be drawn for processing glass batch in industrial glass tanks,

Received November 8, 1991.

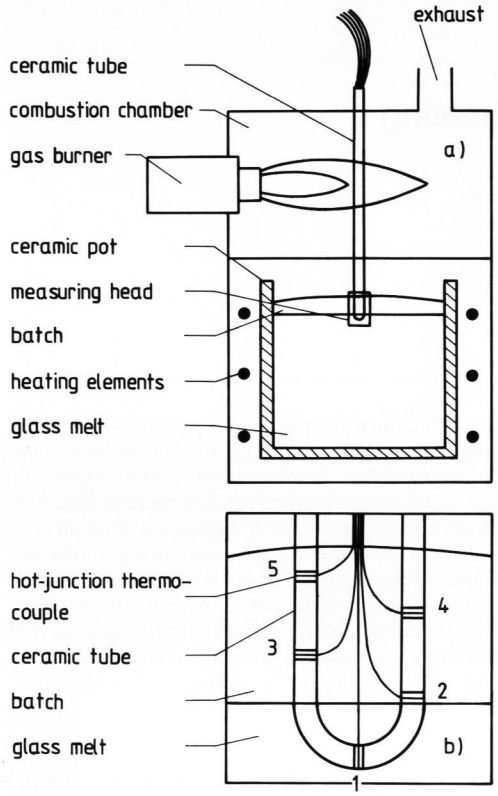

Figures 1a and b. Experimental setup of a studio furnace for batch heating measurements (figure a) and the arrangement of a number of thermocouples in the measuring head of the ceramic tube (figure b).

Table 1. Overview of batch heating experiments

no.	type of batch blanket	ϑ_{melt} in °C	ϑ_{chamb} in °C
1	6 kg powder batch (2 wt% H_2O)	1200	1200
2	12 kg powder batch	1200	1200
3	3 kg powder/3 kg cullet	1200	1200
4	6 kg cullet	1200	1200
5	6 kg dried batch (0 wt% H_2O)	1200	1200
6	6 kg wetted batch (4 wt% H_2O)	1200	1200
7	5 kg pellets	1200	1200
8	6 kg powder batch	1400	1200
9	6 kg powder batch	1200	1400
10	6 kg powder batch	1400	1400
11	6 kg quartz sand	1400	1400

including practical recommendations for preparation, feeding and heating of glass batch materials.

2. Experimental

The measurements have been carried out in a studio furnace, consisting of two parts (figure 1a). The lower part is electrically heated by SiC elements with a total power of 20 kW and contains a ceramic pot with a volume of 40 l. This pot is partly filled with a glass melt. The upper part of the furnace is heated by a natural gas-fired burner. Combustion chamber temperature and pot temperature are controlled independently. A hole has been drilled in the refractory of the top of the furnace, through which an Al_2O_3 tube with five or six thermocouples can be introduced vertically from the top and positioned in a batch layer, just above the glass level (figure 1b). The hot junctions of the Pt-Pt/Rh (S-type) thermocouples are fixed in small holes in the wall of the ceramic tube at every 2 or 2.5 cm in height.

The ceramic tube used is of a porous quality (80 wt% Al_2O_3) and has a low thermal conductivity of 1.4 W/(m · K) up to 100 °C. At higher temperatures the conductivity of the Al_2O_3 tube is even lower, so that the heat flow through its wall (wall thickness: 2.5 mm) is negligible.

At the start of an experiment, the batch is charged on the glass melt with help of a special metal container. This container can be entered through the front door into the upper part of the furnace and emptied above the melt within 30 s in such a way that a reasonably homogeneous batch blanket is obtained. For a central batch thickness of 8 cm, a batch weight of approximately 6 kg is needed. After the batch has been brought in, the measuring head with the multi-thermocouple is positioned in the batch and the temperature distribution in the batch in the vertical direction is recorded as a function of time, t.

The glass batch that has been studied most extensively has a barium–strontium composition. However, it appeared from preliminary experiments with float glass batch that the qualitative thermal behaviour of this batch type is very similar. The batch parameters that have been varied include:

a) weight of batch fed into furnace: 6 and 12 kg,

b) cullet fraction: 0, 50 and 100 wt% cullet (size < 8 mm),

c) water content: 0, 2 and 4 wt%,

d) 100 % pellets (size 0.5 to 2 cm).

In a control experiment a 100 % quartz grain batch was charged on the melt (grain size: 100 to 300 µm, average diameter: 200 µm).

The following furnace temperature conditions have been applied for ϑ_{melt} and ϑ_{chamb} (in °C): $\vartheta_{melt}/\vartheta_{chamb}$ = 1200/1200; 1400/1200; 1200/1400 and 1400/1400, respectively. The batch and furnace conditions for a number of experiments are summarized in table 1.

3. Results and discussion

3.1. Time-dependent batch temperature distributions and influences of different parameters

3.1.1. Influence of layer thickness

In figure 2 the temperature-time curves at different positions in a 6 kg glass batch are shown. The time $t = 0$ corresponds to the moment of charging the batch. During the experiment the temperature of

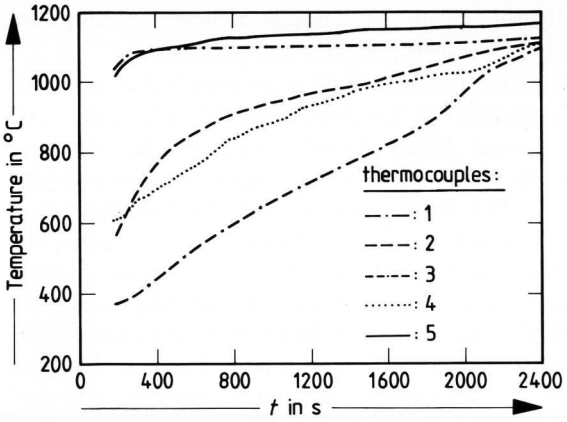

Figure 2. Temperature evolution at different vertical positions in a 6 kg barium–strontium powder batch layer (experiment no. 1 with 2 wt% H_2O) at an oven temperature of 1200 °C for a number of thermocouples.

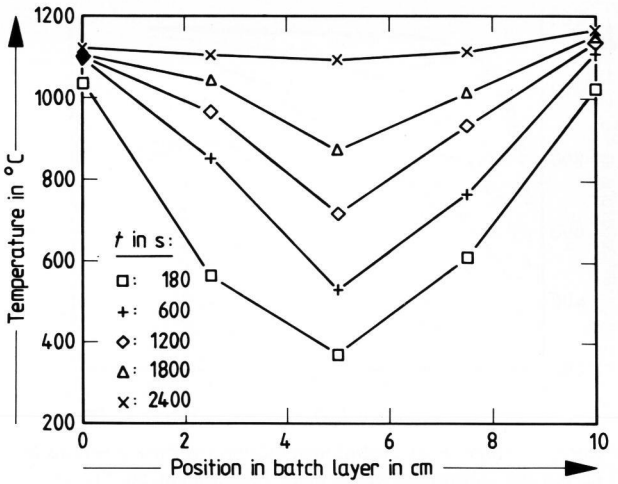

Figure 3. Temperature distributions of a 6 kg barium–strontium powder batch layer during heating (experiment no. 1 with 2 wt% H_2O) as a function of a the thermocouple positions in the batch layer and with record time, t, as parameter.

both the combustion chamber of the furnace and the ceramic pot were maintained at 1200 °C. Thermocouple no. 1 was positioned in the bottom layer of the batch (melt side), thermocouple no. 5 in the top layer (furnace side), see figure 1b.

The resulting temperature distributions in the batch at 5 different times after charging are presented by figure 3. The position $x = 0$ cm corresponds to the melt/batch interface; the position $x = 10$ cm to the batch/combustion chamber interface. The temperature distribution in the batch appears to be almost symmetrical just after charging ($t = 180$ s). However, after some time the temperature at position 2 (melt side) becomes somewhat higher than the temperature at position 4 (furnace side). This implies that the total (conductive and radiative) heat transport from the melt to the batch is higher than the radiative transport from the combustion space, which appears to be in agreement with earlier studies [2 and 3].

To study the influence of the layer thickness, the experiment was repeated for a 12 kg batch, having an initial central thickness of about 16 cm (these curves are not shown here). The heating of the 12 kg batch lasts much longer than that of the 6 kg batch. In fact, the time t for the inner layer of the 12 kg batch to reach 800 °C differs almost by a factor of 4 in comparison with the 6 kg batch layer:

$$\frac{t_{12\,\mathrm{kg}}\ (\vartheta_s = 800\ °\mathrm{C}),}{t_{6\,\mathrm{kg}}\ (\vartheta_s = 800\ °\mathrm{C}),} = 5450/1550 \approx 3.5\ .$$

3.1.2. Influence of cullet fraction, water content, pelletizing and furnace temperatures

Temperature-time curves were also measured for a 50 % cullet/50 % batch (not shown here) and for a 100 % cullet layer under otherwise similar conditions (figure 4). By comparing figures 2 and 4 it can be seen that the cullet layer heats up much more rapidly (by a factor of 1.6 to 1.7) than the pure batch layer. This is

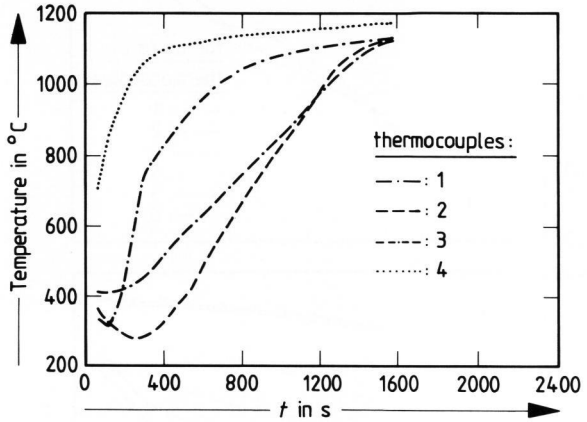

Figure 4. Temperature evolution at different vertical positions in a 6 kg cullet layer (experiment no. 4) as a function of the charging time, t, after charging for a number of thermocouples.

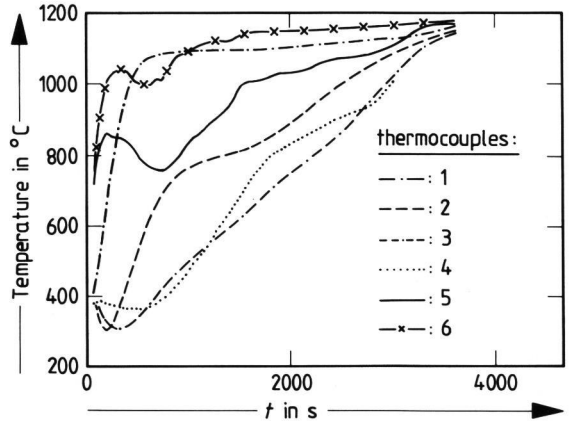

Figure 5. Temperature evolution at different vertical positions in a 6 kg wetted barium–strontium batch layer (experiment no. 6) as a function of time, t, after charging.

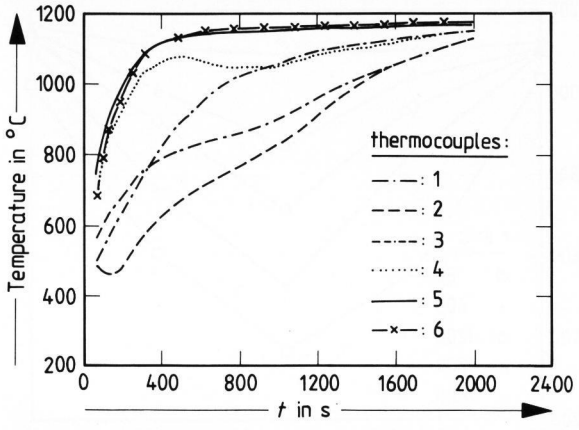

Figure 6. Temperature evolution at different vertical positions in a 5 kg barium–strontium pellet layer (experiment no. 7).

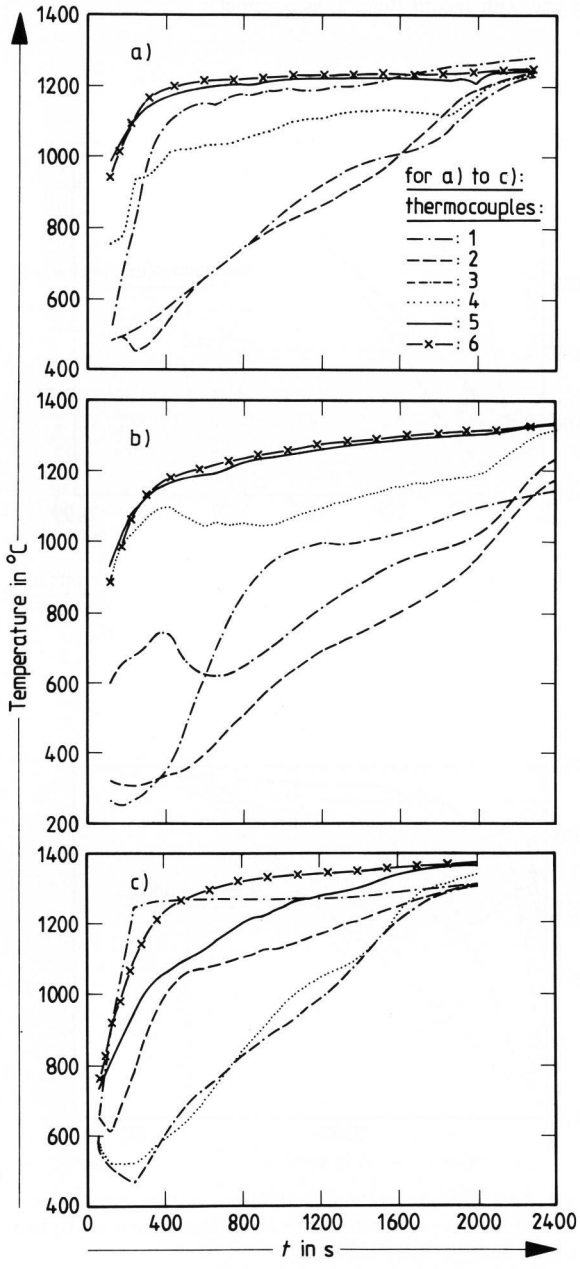

Figures 7a to c. Temperature evolution at different vertical positions in a 6 kg standard (barium–strontium) batch layer with a) $\vartheta_{melt} = 1400\,°C$ (experiment no. 8), b) $\vartheta_{chamb} = 1400\,°C$ (experiment no. 9), c) $\vartheta_{melt} = \vartheta_{chamb} = 1400\,°C$ (experiment no. 10).

partly caused by the absence of heat consumption, needed for fusion, in the cullet layer.

Similar measurements as for pure batch and cullet were carried out for dried batch (0 wt% water) and for wetted batch (4 wt% water). The standard (powder) batch has a water content of approximately 2 wt%. The thermal behaviour of the dried batch was identical to the standard batch. Figure 5 shows the temperature-time curves for a 6 kg wetted (4 wt% water) batch layer, heated to a temperature of 1200 °C from both sides. In figure 5, the furnace-side batch layers (curves for thermocouples no. 5 and 6) show a temperature minimum between 500 and 1000 s after batch charging. This could be caused by the extra heat absorption needed for the evaporation of the water. By comparing figure 5 to figure 2 it appears that the heating rate of the wetted batch layer is lower than that of the standard (powder) batch by about 50 %.

In figure 6 the temperature-time curves of a 5 kg pellet layer (thickness ≈ 7 cm) are shown, heated from two sides at 1200 °C. The heating rate of the 5 kg pellet layer is (ca. 40 %) higher than the rate of the 6 kg (powder) batch layer. This difference in heating rate is mainly a result of the difference in weight between the two batches, as will be illustrated in section 4.

The heating curves of 6 kg powder batch for different furnace temperature conditions are depicted in figures 7a to c. By comparing these figures it can be concluded that increasing the glass melt temperature from 1200 to 1400 °C accelerates the heating of the batch by approximately 40 %. Increasing only the combustion chamber temperature from 1200 to 1400 °C and leaving the glass melt temperature at 1200 °C, does not effectively result in a higher heating rate. This is caused by the better (conductive plus radiative) heat transport from the melt side to the batch in comparison to the radiative transfer from the combustion side (see section 3.1.1.). Partly, it can be due to the heat-screening effect of a more fastly developing scum layer on the batch in the latter case as well.

3.1.3. Heating of pure quartz layer instead of batch

In a control experiment, a 6 kg pure quartz layer was charged on the glass melt at 1400 °C, with a combustion chamber temperature of 1400 °C as well. The density of the quartz powder (grain size: 100 to 300 μm, average diameter: 200 μm) is a factor 0.8

lower than of the barium–strontium glass batch, so the central quartz layer has a thickness of about 0.10 m. Again, the time-dependent temperature distribution in the batch was measured. The resulting temperature curves are shown in figure 8. Obviously, the heating rate of the quartz layer is much lower than the heating rate of the batch layer in figure 7c, recorded under the same furnace temperature conditions. This is explained by two effects:

a) the quartz layer is 20 % thicker than the batch layer,

b) in the quartz layer no glassy phases arise which normally increase the thermal diffusivity.

3.2. Determination of the virtual thermal diffusivity

The virtual thermal diffusivity $a = \lambda/(\varrho \cdot c_p)$, where λ is the thermal conductivity, ϱ is the density and c_p the specific heat of a batch layer as a function of temperature can be obtained by discretization of the one-dimensional Fourier equation with data from the heating curves of section 3.1. as follows:

$$a(\vartheta_{m,t}) = \frac{(\Delta x^2/\Delta t) \cdot (\vartheta_{m,t+\Delta t} - \vartheta_{m,t})}{(\vartheta_{m-1,t} + \vartheta_{m+1,t} - 2\vartheta_{m,t})}, \qquad (1)$$

where Δx = distance (in m) between neighbouring thermocouples, Δt = time interval (in s) between successive measurements, $\vartheta_{m,t}$ = temperature (in °C) at position (thermocouple) m at moment t, $\vartheta_{m,t+\Delta t}$ = temperature (in °C) at position (thermocouple) m at moment $t + \Delta t$, $\vartheta_{m-1,t}$ = temperature (in °C) at position (thermocouple) $m - 1$ at moment t, $\vartheta_{m+1,t}$ = temperature (in °C) at position (thermocouple) $m + 1$ at moment t. The result of this calculation for the experiments 1, 3 and 4 (see table 1) is shown in figure 9a. It can be seen in this figure that the virtual thermal diffusivity of a pure batch layer remains almost constant up to 900 °C at a value of approximately $0.4 \cdot 10^{-6}$ m²/s. Above 900 °C the thermal diffusivity rises steeply. The thermal diffusivity of a 100 % cullet layer increases slowly from $0.4 \cdot 10^{-6}$ m²/s at 500 °C to about $0.9 \cdot 10^{-6}$ m²/s at 900 °C. Above 900 °C the thermal diffusivity of the cullet rises steeply as well. However, the virtual thermal diffusivity curves of the 100 % cullet layer and the 100 % batch layer do not coincide in the temperature region above 900 °C, due to different physical properties, e.g. the formation of scum in the powder batch.

The virtual thermal diffusivity of a 50 % batch/50 % cullet layer is very similar to that of a pure batch layer up to 900 °C. Apparently, there is hardly or no effect of the cullet fraction on the thermal diffusivity in this temperature region for a cullet fraction of 50 % or less. Beyond 900 °C the batch/cullet layer shows an intermediate behaviour between the 100 % batch and the 100 % cullet layer.

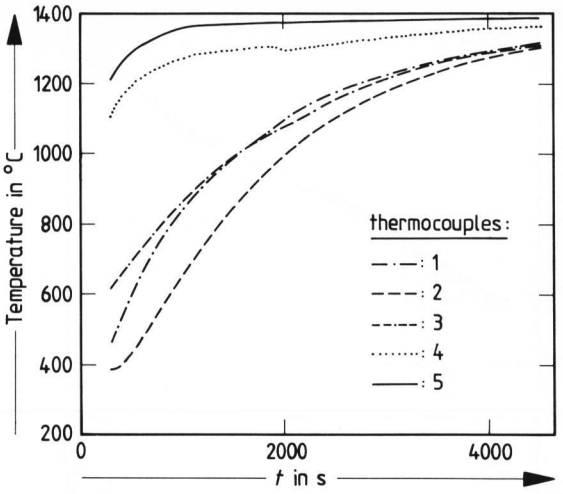

Figure 8. Temperature evolution at different vertical positions in a 6 kg quartz sand layer (experiment no. 11).

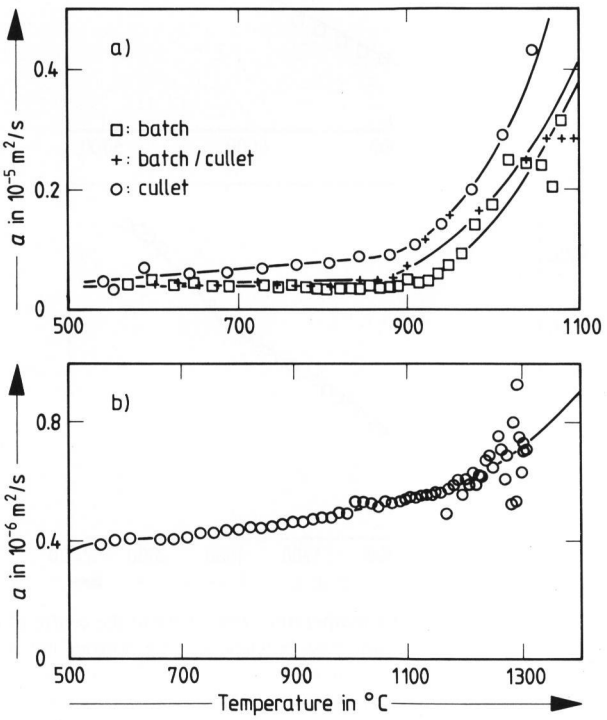

Figures 9a and b. Virtual thermal diffusivity, a, as a function of temperature for a) three types of batch blankets (□: 100 % standard powder batch, +: 50 % powder batch/50 % cullet, ○: 100 % cullet), b) quartz sand (average grain diameter = 200 μm).

Surprisingly, the virtual thermal diffusivities determined as functions of temperature for both the wet (4 wt% water) and the pellet layer (curves not shown here) are very similar to the curve for normal batch. Wetting or pelletizing the batch hardly influences the effective thermal diffusivity of the batch. The temperature-dependent thermal diffusivity of the quartz powder layer, calculated with data of figure 8, is given in figure 9b. This figure shows a slowly but

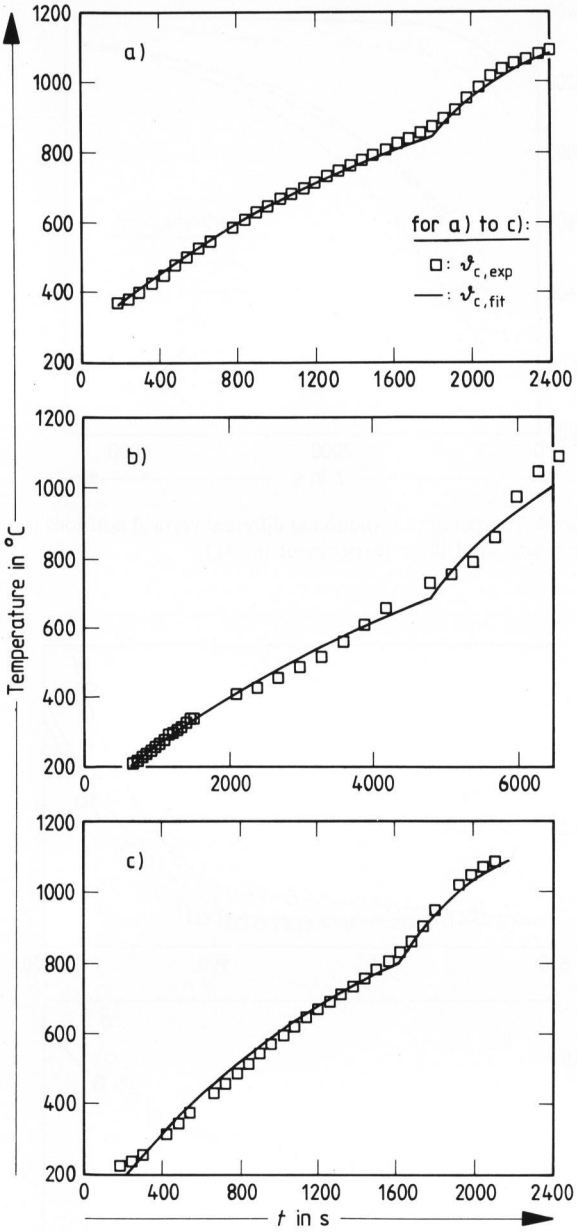

Figures 10a to c. Fit of the temperature-time curve at the centre of different barium–strontium glass batches; a) 6 kg powder batch layer with the parameter values $a_1 = 0.4 \cdot 10^{-6}$ m²/s, $a_2 = 1.0 \cdot 10^{-6}$ m²/s, $d = 0.09$ m, $\vartheta_0 = 280$ °C, $\vartheta_b = \vartheta_{top} = 1200$ °C, $\vartheta_s = 840$ °C; b) 12 kg powder batch layer with the parameter values $a_1 = 0.4 \cdot 10^{-6}$ m²/s, $a_2 = 1.0 \cdot 10^{-6}$ m²/s, $d = 0.16$ m, $\vartheta_0 = 100$ °C, $\vartheta_b = \vartheta_{top} = 1200$ °C, $\vartheta_s = 690$ °C; c) 6 kg (50 % powder/50 % cullet) batch with the parameter values $a_1 = 0.4 \cdot 10^{-6}$ m²/s, $a_2 = 1.0 \cdot 10^{-6}$ m²/s, $d = 0.08$ m, $\vartheta_0 = 50$ °C, $\vartheta_b = \vartheta_{top} = 1200$ °C, $\vartheta_s = 800$ °C.

continuously rising function, as expected, increasing from a value of ca. $0.4 \cdot 10^{-6}$ m²/s at 500 °C to approximately $0.7 \cdot 10^{-6}$ m²/s at 1300 °C.

4. Modelling

4.1. Description of model

Assuming a heat penetration model, the time-dependent minimum temperature, ϑ_c, at the centre of an infinite slab of an isotropic material with thermal diffusivity, a, and thickness, d, heated from two sides starting at time $t = 0$, can be calculated by the following equation [5]:

$$\vartheta_c = (\vartheta_b + \vartheta_{top})/2 + (\vartheta_0 - (\vartheta_b + \vartheta_{top})/2)) \cdot \cdot \exp(-\pi^2 a\, t/d^2)\,, \quad (2)$$

where ϑ_b = temperature at bottom of slab, ϑ_{top} = temperature at top of slab, ϑ_0 = initial slab temperature.

In the model it is assumed that the glass batch layer can be considered as an infinite slab with thermal diffusivity a_1 until the whole batch has reached a certain 'batch transition' temperature, ϑ_s. This batch transition corresponds to the onset of the actual melting process, involving the melting of the alkali components in the batch and resulting in the formation of primary transparent glassy phases. So, the batch transition temperature lies in the range between 700 and 900 °C. It is assumed further that for temperatures $\vartheta > \vartheta_s$, the virtual thermal diffusivity of the batch can be described by: $a_n = a_1 + a_2$, where a_2 is the contribution of the molten phases in the batch to the net thermal diffusivity. In summary, the inner batch temperature can thus be described by the following two equations:

for $\vartheta < \vartheta_s$

$$\vartheta_c = (\vartheta_b + \vartheta_{top})/2 + (\vartheta_0 - (\vartheta_b + \vartheta_{top})/2) \cdot \cdot \exp(-\pi^2 a_1\, t/d^2)\,, \quad (3)$$

and for $\vartheta > \vartheta_s$

$$\vartheta_c = (\vartheta_b + \vartheta_{top})/2 + (\vartheta_0 - (\vartheta_b + \vartheta_{top})/2) \cdot \cdot \exp(-\pi^2 (a_n\, t - a_2\, t_s)/d^2)\,, \quad (4)$$

where the subscripts c, b, top and 0 have the same meaning as in equation (2) with 'slab' replaced by batch layer, where t is the time passed after the moment of charging and where t_s is the required time for the batch to reach ϑ_s. The equations (3 and 4) are based on a simplified description of the complex heating process of a batch blanket. More sophisticated mathematical models, that take into account continuously varying batch properties, inner heat sources and gas percolation in the batch are described in the literature, see e.g. [6]. However, in section 4.2. it will be shown that the results of the semi-empirical model are in satisfactory agreement with the experiments so that the simplifications of this model appear to be justified.

4.2. Verification of model by fitting experimental curves

The equations (3 and 4) are verified by fitting the experimental curves for the temperature evolution of the inner batch layer of section 3.1., using the

semi-empirical values for the virtual thermal diffusivity, found in section 3.2.

The results of the fitting procedure, including the fitting parameters a_1, a_2, d, ϑ_0, ϑ_b, ϑ_{top}, and ϑ_s, are shown in figures 10a to c through 13. With regard to these figures the following remarks can be made:

a) Generally, the agreement between theoretical curves and experimental data is very good. This supports the assumption that batch heating can be described by a heat penetration model.

b) The experimental heating curve of the 6 kg standard batch layer (figure 10a) is well approximated by the equations (3 and 4), with the following parameter values:

- $a_1 = 0.4 \cdot 10^{-6}$ m²/s, on the basis of experiments (see section 3.2.);
- $\vartheta_s \approx 840$ °C and $t_s = 1800$ s, by a 'qualitative best fit' procedure;
- $a_2 = 1.0 \cdot 10^{-6}$ m²/s, an estimated average value for $\vartheta_s < \vartheta < 1100$ °C with reference to figure 9a. Of course, in fact this parameter is strongly temperature-dependent (figure 9a);
- $d \approx 0.087$ m, within 10 % of the estimated value (0.08 m);
- $(\vartheta_b + \vartheta_{top})/2 = 1200$ °C, on the basis of the actual furnace temperatures;
- $\vartheta_0 = 280$ °C, by extrapolating the experimental curve to $t = 0$; ϑ_0 differs from room temperature because the thermocouple tube has an initial temperature equal to the furnace temperature so that ϑ_0 is the temperature at which the thermocouple tube and the cold batch reach thermal equilibrium.

c) The effect of layer thickness is readily accounted for by the thickness parameter d: $d = 0.16$ m for a 12 kg batch (figure 10b).

d) The influence of 100 % cullet (figure 11a) is accounted for by the thermal diffusivity parameter a_1: $a_1 = 0.6 \cdot 10^{-6}$ m²/s (average value) for a 100 % cullet layer (see figure 9a). Since it was found in section 3.2. that a_1 of the 50 % batch/50 % cullet layer is approximately the same as that of the 100 % batch layer (figure 9a) the heating curves of these two batch types are virtually identical (see figure 10c).

e) Fitting the heating curve of the wetted batch layer, a value for a_1 of $0.4 \cdot 10^{-6}$ m²/s as for standard batch is used, in view of experimental results (see section 3.2.). To account for the slower heating rate of the wetted batch, the parameter d was increased to 0.1 m, representing an "effective thickness" of the wetted batch layer (figure 11b).

f) The heating curve of the 5 kg pellet layer is fitted by using a value for a_1 of $0.4 \cdot 10^{-6}$ m²/s, also on the basis of experimental results (section 3.2.), and a thickness d of $(5/6) \cdot 8$ cm ≈ 7 cm (figure 11c).

g) The values for ϑ_s of the different batch types, heated at 1200 °C, are all in the range between 800 and 900 °C; no unambiguous dependence of ϑ_s on batch type has been found. Obviously, for $\vartheta < 800$ °C, heat penetration is the determining process during batch heating, rather than chemical reactions.

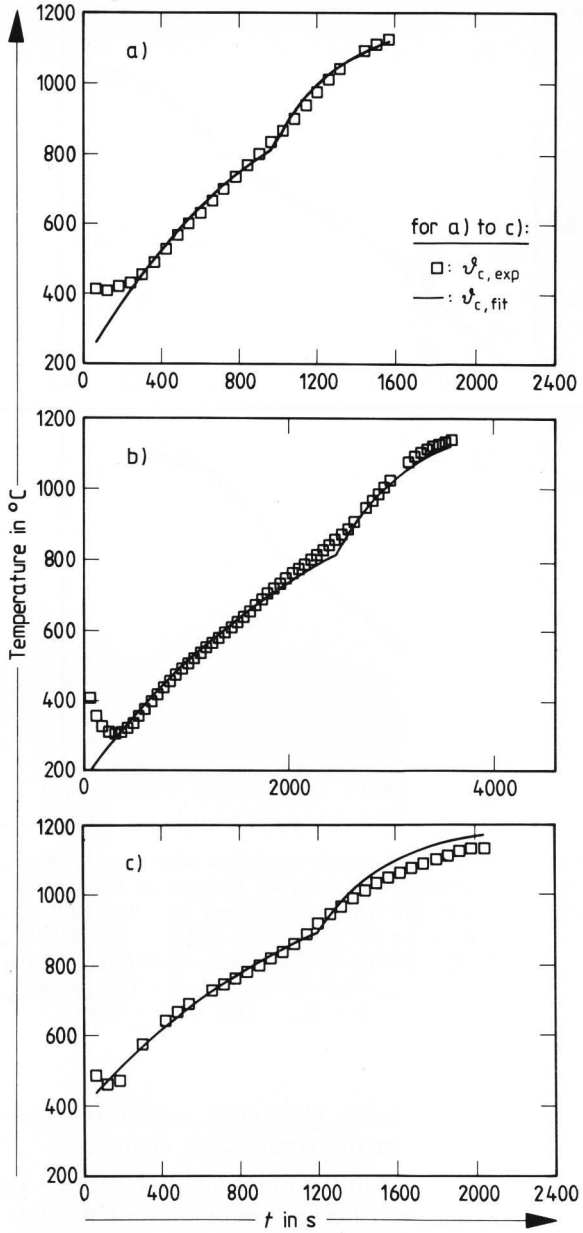

Figures 11a to c. Fit of temperature-time curves at the centre of different barium–strontium glass batches; a) 6 kg cullet batch layer with the parameter values $a_1 = 0.6 \cdot 10^{-6}$ m²/s, $a_2 = 1.0 \cdot 10^{-6}$ m²/s, $d = 0.08$ m, $\vartheta_0 = 200$ °C, $\vartheta_b = \vartheta_{top} = 1200$ °C, $\vartheta_s = 810$ °C; b) 6 kg wetted batch layer (4 wt% H_2O) with the parameter values $a_1 = 0.4 \cdot 10^{-6}$ m²/s, $a_2 = 1.0 \cdot 10^{-6}$ m²/s, $d = 0.1$ m, $\vartheta_0 = 175$ °C, $\vartheta_b = \vartheta_{top} = 1200$ °C, $\vartheta_s = 810$ °C; c) 5 kg pellet layer with the parameter values $a_1 = 0.4 \cdot 10^{-6}$ m²/s, $a_2 = 1.0 \cdot 10^{-6}$ m²/s, $d = 0.07$ m, $\vartheta_0 = 400$ °C, $\vartheta_b = \vartheta_{top} = 1200$ °C, $\vartheta_s = 890$ °C.

h) The effects of higher furnace temperatures are accounted for by the temperature parameters ϑ_t and ϑ_b (figures 12 a and b). However, the model does not discriminate between the (conductive and radiative)

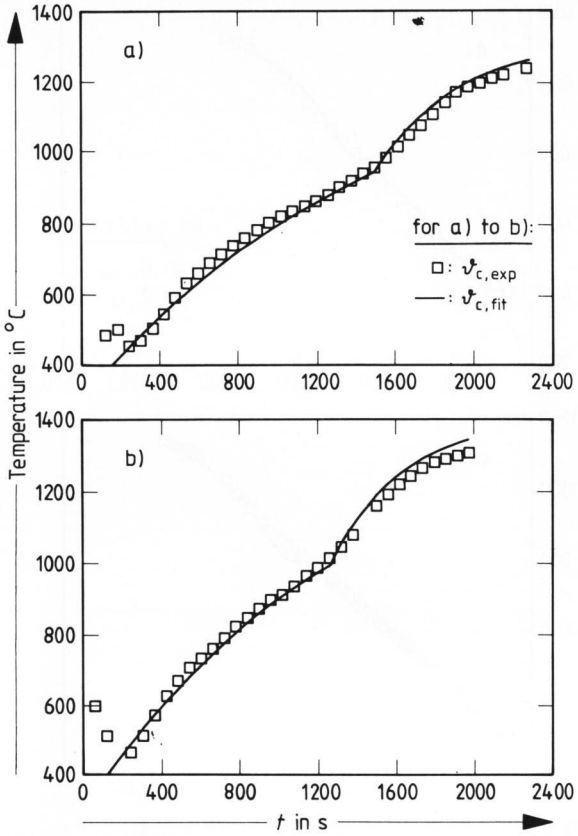

Figures 12a to c. Fit of temperature-time curves at the centre of different barium–strontium glass batches; a) 6 kg powder batch layer with the parameter values $a_1 = 0.4 \cdot 10^{-6}$ m²/s, $a_2 = 1.0 \cdot 10^{-6}$ m²/s, $d = 0.08$ m, $\vartheta_0 = 280$ °C, $\vartheta_b = 1400$ °C, $\vartheta_{top} = 1200$ °C, $\vartheta_s = 940$ °C; b) 6 kg powder batch layer with the parameter values $a_1 = 0.4 \cdot 10^{-6}$ m²/s, $a_2 = 1.0 \cdot 10^{-6}$ m²/s, $d = 0.07$ m, $\vartheta_0 = 300$ °C, $\vartheta_b = \vartheta_{top} = 1400$ °C, $\vartheta_s = 990$ °C.

heat transport from the glass melt and the radiative heat transport from the combustion chamber.

i) The heating curve at the inner quartz layer of 6 kg is approximated by using the temperature-dependent thermal diffusivity curve $a(\vartheta)$ of figure 9b and an actual thickness of 0.1 m (figure 13). Of course, in the case of the quartz layer no batch transition due to the occurrence of low-melting phases is taken into account.

5. Relation to melting kinetics models and future work

During the heating of the batch blanket of raw materials, chemical reactions take place depending on the local composition of the batch and the local temperature. At a certain temperature, liquid melting phases will occur and dissociation of for example carbonates, nitrates and sulphates will lead to the evolution of gases from the batch blanket. The processes in this stage are very complex and an accurate quantitative description of the conversions of batch into a melt is very difficult.

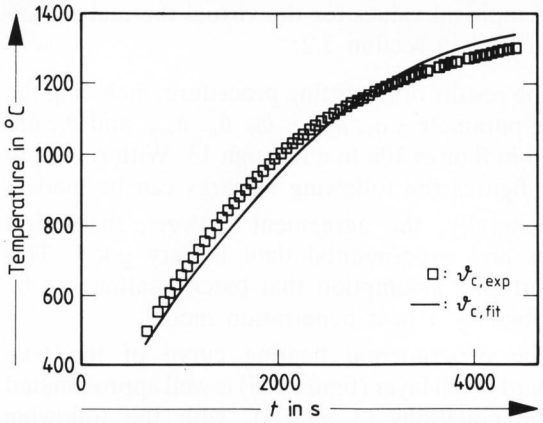

Figure 13. Fit of the temperature-time curve at the centre of a 6 kg quartz sand layer with the parameter values $a(<\vartheta>) = -3.0 \cdot 10^{-7} + <\vartheta> 2.5 \cdot 10^{-9} - <\vartheta^2> 3.0 \cdot 10^{-12} + + <\vartheta^3> 1.3 \cdot 10^{-15}$ m²/s, with $<\vartheta>$ = the average temperature in the central sand layers at time $t - \Delta t$, $d = 0.1$ m, $\vartheta_0 = 200$ °C, $\vartheta_b = \vartheta_{top} = 1400$ °C.

For example for soda–lime batches, at first a liquid phase is formed, which is rich in calcium and sodium oxides. Above 1100 °C only sand grains are not completely dissolved in this melt; the other components react very fast at these temperature levels and are dissolved completely. The dissolution of the remaining sand grains at temperatures above 1100 °C is important for obtaining a homogeneous melt without grains.

The dissolution of mono-sized sand grains in isothermally heated batch has been described by Mühlbauer and Němec [7] and experiments have been carried out for soda–lime–silica glass batch by Benes [8]. A semi-empirical model suitable for non-isothermal situations has been proposed by Beerkens [9]. The dissolution kinetics of sand grains of different sizes can be described for the batch blanket situation above 1100 °C as a function of the temperature and the course of the melting process. The model describes the decrease of the diameter of sand grains for different size classes and depending on the temperature course and the already dissolved amount of sand. As the dissolution proceeds, the silica content of the melt increases which leads to a decrease in the solubility of the remaining undissolved SiO_2 in the liquid phase. Otherwise the solubility and diffusivity of SiO_2 in the melt increases with the temperature. The sand dissolution model considers these effects: The amount of dissolved SiO_2 is calculated during the melting process and from this the driving force $(C_i - C_w)$ for dissolution can be derived, where C_i = the concentration of SiO_2 in the melt at the interface with the sand grain and C_w = the concentration of this component in the bulk of the melt. The value of C_w depends on the amount of sand already dissolved, the value of C_i is determined by the thermodynamics of SiO_2 in soda–lime melts. Detailed information of the derivation of C_i, C_w and the

dissolution rate dR/dt (decrease of sand grain radius, R) which is proportional to $(C_i - C_w)$ and the diffusivity is given in [9].

By a combination of the sand dissolution model with the present heat penetration batch blanket model it will be possible to calculate the kinetics of melting during the heating of the batch. The combined model directly calculates the local amount of undissolved sand during batch blanket heating. Thus, it is possible to determine the locations in the batch blanket where sand dissolution takes place and the local state of the batch blanket. Future work will be focused on the integration of the heat transfer model and the sand dissolution model in glass tank modelling.

6. Conclusions and recommendations

In conclusion it can be stated that a two-stage heat penetration model for glass batch, considered as an infinite slab heated from two sides, gives a fairly good approximation of its thermal behaviour during heating and melting down (up to 1100 °C). Below a certain batch transition temperature, ϑ_s, (typically from 700 to 900 °C) the thermal diffusivity of barium–strontium glass batch has a value of approximately $0.4 \cdot 10^{-6}$ m²/s. At higher temperatures than ϑ_s, low-melting glassy phases also contribute to the net thermal diffusivity, resulting in a virtual value of $1.4 \cdot 10^{-6}$ m²/s for 100 % batch in the temperature region $\vartheta_s < \vartheta < 1100$ °C.

The batch model described here, can cope with the effects of several batch characteristics, including layer thickness and composition (cullet fraction, water content, pellets) and with the influence of the temperature conditions. By combining experimental data and model it is concluded that layer thickness and cullet fraction have a major effect on the heating rate of glass batch but pellets only have a minor effect. However, the beneficial effect of cullet on batch heating only becomes apparent for cullet fractions higher than 50 %. Furthermore, wetting the batch to a surplus water content of 4 wt% gives no increase of the virtual thermal diffusivity, but on the contrary it has a retarding effect on the heating rate due to extra heat consumption by water. It appears that increasing the temperature of the glass melt is more effective for improving the batch heating rate than increasing the temperature of the combustion chamber.

Summarizing, for accelerating the heating and melting down of glass batch in industrial glass tanks, it is recommended to use batch with a cullet fraction as high as possible, to feed the furnace with thin batch blankets, and to operate the furnace in such a way that much heat is supplied from the lower (melt) side of the batch.

*

The authors are grateful to Philips' Technology Centre Glass, Eindhoven (NL), for the supply of the batch materials. The financial support from NOVEM (Nederlandse Organisatie voor Energie en Milieu), Sittard (NL), is greatly appreciated.

7. References

[1] Kröger, C.; Eligehausen, H.: Über das Wärmeleitvermögen des einschmelzenden Glasgemenges. Glastech. Ber. **32** (1959) no. 9, p. 362–373.

[2] Daniels, M.: Einschmelzverhalten von Glasgemengen. Glastech. Ber. **46** (1973) no. 3, p. 40–46.

[3] Costa, P.: Untersuchung des Einschmelzverhaltens von pelletiertem Gemenge zur Glasherstellung. Glastech. Ber. **50** (1977) no. 1, p. 10–18.

[4] Jack, H. R. S.; Jacquest, J. A. T.: Heat transfer in glass-batch materials. In: Symposium sur la fusion du verre, Bruxelles 1958. C. r. Charleroi: Union Scientifique Continental du Verre 1958. p. 339–360.

[5] Carslaw, H. S.; Jaeger, J. C.: Conduction of heat in solids. London: Oxford Univ. Press 1959.

[6] Fuhrmann, H.: Beitrag zur näherungsweisen Berechnung des Abschmelzens von Glasgemengeschichten. T. 1. Theoretische Ableitungen. T. 2. Numerische Ergebnisse. Glastech. Ber. **46** (1973) no. 10, p. 201–208; no. 11, p. 209–218.

[7] Mühlbauer, M.; Němec, L.: Dissolution of glass sand. Am. Ceram. Soc. Bull. **64** (1985) no. 11, p. 1471–1475.

[8] Benes, J.: The kinetics of silicate glass melting. Institute of Chemical Technology, Prague, thesis 1977.

[9] Beerkens, R. G. C.: Kinetik der Quarzsandauflösung in Gemengeteppich und in Glasschmelzen. In: 63. Glastechnische Tagung, Stuttgart 1989. Kurzreferate. Frankfurt/M.: Deutsche Glastechnische Gesellschaft 1989. p. 65–70.

92R0559